Eur. Phys. J. C 46, 729–739 (2006)
Digital Object Identifier (DOI) 10.1140/epjc/s2006-02529-3

THE EUROPEAN PHYSICAL JOURNAL C

Can the total angular momentum of u-quarks in the nucleon be accessed at HERMES?

F. Ellinghaus[1], W.-D. Nowak[2], A.V. Vinnikov[2,3,a], Z. Ye[4]

[1] Department of Physics, University of Colorado, Boulder, Colorado 80309-0390, USA
[2] DESY, 15738 Zeuthen, Germany
[3] BLTP JINR, 141980, Dubna, Moscow region, Russia
[4] DESY, 22603 Hamburg, Germany

Received: 2 September 2005 / Revised version: 17 February 2006 /
Published online: 31 March 2006 – © Springer-Verlag / Società Italiana di Fisica 2006

Abstract. We investigate the possibility of acquiring information on the generalized parton distribution E and, through a model for E, also on the u-quark total angular momentum J_u by studying deeply virtual Compton scattering and hard exclusive ρ^0 electroproduction on a transversely polarized hydrogen target at HERMES. It is found that a change in J_u from zero to 0.4 corresponds to a 4σ (2σ) difference in the calculated transverse target-spin asymmetry in deeply virtual Compton scattering (ρ^0 electroproduction), where σ is the total experimental uncertainty.

PACS. 12.38.Bx; 13.60.Le

1 Introduction

Over more than 2 decades, inclusive and semi-inclusive charged lepton scattering has been used as a powerful tool to successfully study the longitudinal momentum structure of the nucleon, which was parameterized in terms of parton distribution functions (PDFs). Hard exclusive reactions can be described in the theoretical framework of generalized parton distributions (GPDs) [1–5]. Their application became apparent after it was shown [6] that measurements of the second moment of the sum of the "unpolarized" GPDs H and E open, for the first time, access to the total angular momentum of partons in the nucleon:

$$J_{\mathrm{a}}(Q^2) = \frac{1}{2}\lim_{t\to 0}\int_{-1}^{1} x\Big[H_{\mathrm{a}}(x,\xi,t,Q^2) + E_{\mathrm{a}}(x,\xi,t,Q^2)\Big]\,\mathrm{d}x\,. \tag{1}$$

In this relation, also known as the Ji sum rule, $H_{\mathrm{a}}(x,\xi,t,Q^2)$ and $E_{\mathrm{a}}(x,\xi,t,Q^2)$ denote parton spin-nonflip and spin-flip GPDs ($a = u,d,s$), respectively.[1] GPDs depend on the fractions x and ξ of longitudinal momentum of the proton carried by the parton and on $t = (p_1 - p_2)^2$, the square of the four-momentum transfer between initial and final protons (Fig. 1). As ordinary PDFs, GPDs are also subject to QCD evolution. Their Q^2 dependence has been perturbatively calculated up to next-to-leading order in α_{s} [8] and is omitted in the notations throughout the paper.

Recently, a simultaneous description of the transverse spatial and the longitudinal momentum structure of the nucleon was shown to be an appealing interpretation of GPDs [9–12]. The concept of GPDs covers several types of processes, ranging from inclusive deeply inelastic lepton scattering to hard exclusive Compton scattering and meson production. Measurements of GPDs are expected to shed light especially on the hitherto theoretically uncharted territory of long-range ("soft") phenomena where parton–parton correlations are known to play an important role.

A drawback in the determination of GPDs from data on hard exclusive reactions is the model dependence of the extraction procedure. Indeed, in distinction from ordinary

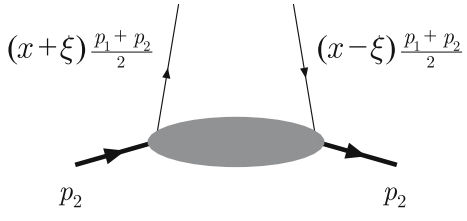

Fig. 1. In the parton picture, GPDs describe correlations between two partons with different longitudinal momenta at given Q^2 and t, where $t = (p_1 - p_2)^2$ also contains transverse degrees of freedom

[a] e-mail: vinnikov@ifh.de

[1] Throughout this paper the GPD definitions of a recent review [7] are used.

PDFs, the GPDs usually enter into physical observables integrated over one of their variables. Therefore, their functional form cannot be determined from the experiment and has to be imposed based on model expectations. Then, the model parameters can be fitted to the data. The eventual determination of GPDs will require a worldwide combination of data into a global analysis, very much as has been customary for decades in the determination of ordinary PDFs.

The first steps toward the extraction of the GPD H have already been performed by scattering leptons off unpolarized protons through measurements of either cross sections [13, 14] or cross-section asymmetries with respect to beam charge [15] or beam spin [16, 17]. Future measurements of the transverse target-spin asymmetry (TTSA) in hard exclusive electroproduction of a real photon (deeply virtual Compton scattering, DVCS) or a vector meson offer the possibility of acquiring information on the spin-flip GPD E. The most promising experiments to access it are those running at intermediate energy, where the spin-flip amplitude is expected to be sizable, while at higher energies it is suppressed due to s-channel helicity conservation. Thus at present a realistic program may be envisaged for HERMES, CLAS, and, possibly, COMPASS. In this paper the prospects are discussed for HERMES measurements of TTSAs in DVCS and ρ^0 electroproduction and in particular their sensitivity to the u-quark total angular momentum.

2 Modeling generalized parton distributions

GPDs are most commonly parameterized using an ansatz based on double distributions [21, 22] complemented by the D-term [23]. Factorizing out the t-dependence, the nonforward GPDs can be related to the ordinary PDFs and the proton elastic form factors. In this framework [18], the spin-nonflip GPD H is given by

$$H_{q,g}(x,\xi,t) = \frac{1-(1+\kappa_p)t/4m^2}{1-t/4m^2}\frac{H_{q,g}(x,\xi)}{(1-t/0.71)^2}\,, \quad (2)$$

where $\kappa_{\rm p} = 1.793$ is the proton anomalous magnetic moment and m is the proton mass. The neutron Dirac form factor is neglected compared to that of the proton.

For quarks, the t-independent part of the GPDs $H_{\rm q}$ is written as

$$H_{\rm q}(x,\xi) \;=\; H_{\rm q}^{DD}(x,\xi) + \theta(\xi-|x|) D_{\rm q}\left(\frac{x}{\xi}\right)\,, \quad (3)$$

where $D_{\rm q}\left(\frac{x}{\xi}\right)$ is the D-term and $H_{\rm q}^{DD}$ is the part of the GPD that is obtained from the double distribution (DD) $F_{\rm q}$:

$$H_{\rm q}^{DD}(x,\xi) = \int\limits_{-1}^{1} d\beta \int\limits_{-1+|\beta|}^{1-|\beta|} d\alpha\; \delta(x-\beta-\alpha\xi)\; F_{\rm q}(\beta,\alpha)\,. \quad (4)$$

For the double distributions the suggestion of [21] is used:

$$F_{\rm q}(\beta,\alpha) = h(\beta,\alpha) q(\beta)\,, \quad (5)$$

where the profile function is given by [22]

$$h(\beta,\alpha) = \frac{\Gamma(2b+2)}{2^{2b+1}\Gamma^2(b+1)}\,\frac{\left[(1-|\beta|)^2-\alpha^2\right]^b}{(1-|\beta|)^{2b+1}}\,. \quad (6)$$

For $\beta > 0$, $q(\beta) = q_{\rm val}(\beta) + \bar{q}(\beta)$ is the ordinary quark density for the flavor q. The negative β range corresponds to the antiquark density: $q(-\beta) = -\bar{q}(\beta)$. The parameter b characterizes the extent to which the GPD depends on the skewness ξ. In the limit $b \to \infty$ the GPD is independent of ξ, i.e., $H(x,\xi) = q(x)$. Note that b is a free parameter for valence quarks ($b_{\rm val}$) or sea quarks ($b_{\rm sea}$) and thus can be used as a fit parameter in the extraction of GPDs from hard electroproduction data [24].

For gluons, the t-independent part of the GPD $H_{\rm g}$ is directly given by the double distribution

$$\begin{aligned} H_{\rm g}(x,\xi) &= H_{\rm g}^{DD}(x,\xi) \\ &= \int\limits_{-1}^{1} d\beta \int\limits_{-1+|\beta|}^{1-|\beta|} d\alpha\; \delta(x-\beta-\alpha\xi)\; \beta F_{\rm g}(\beta,\alpha)\,, \end{aligned} \quad (7)$$

with the same form of the profile function in the double distribution

$$F_{\rm g}(\beta,\alpha) = h(\beta,\alpha) g(\beta)\,. \quad (8)$$

The t-dependence for gluons is taken to be the same as that for quarks.

The factorized ansatz (2) is the simplest way of modeling GPDs. However, experimental studies of elastic diffractive processes indicate that the t-dependence of the cross section is entangled with its dependence on the photon–nucleon invariant mass [25]. Recent evidence comes from lattice QCD calculations [26, 27] and phenomenological considerations [19, 20]. The nonfactorized ansatz can be based on soft Regge-type parameterizations. In this case, the t-dependence is not factorized out and not controlled by a form factor as in (2). Instead, it is retained in (3), (4), and (7). The t-dependence of double distributions is then modeled as [18]

$$F_{\rm q,g}(\beta,\alpha,t) = F_{\rm q,g}(\beta,\alpha)\frac{1}{|\beta|^{\alpha' t}}\,, \quad (9)$$

which is referred to as Regge ansatz in what follows. Here α' is the slope of the Regge trajectory, $\alpha'_{\rm q} = 0.8\,{\rm GeV}^{-2}$ for quarks, and $\alpha'_{\rm g} = 0.25\,{\rm GeV}^{-2}$ for gluons.

The other GPD necessary to access the total angular momentum of partons in the nucleon [see (1)] is the GPD E. In the present paper a simple model [18] is used for the parameterization of the spin-flip GPD E. Despite its simplicity, it satisfies the constraint of polinomiality and gives the right values for nucleon magnetic moments. A known drawback of this model is the violation of the positivity

constraints, as described in [19]. However, this violation occurs only for $x > 0.5$ and should therefore have only a slight impact on the calculation of (1); at large values of x the GPDs E and H behave approximately as $(1-x)^3$, i.e., they decrease very rapidly with x. Hence, even though the Ji sum rule represents the integral of $E+H$ weighted with x, the large-x tail of the integral will not be crucial for the sum rule and therefore for the model estimates in this paper. While more sophisticated parameterizations for the GPD E exist (see [19, 20]), the model presented below is the only one where J_u enters directly as a parameter for the GPD E. Therefore, it is anticipated that this model is best suited for the task of estimating the sensitivity of HERMES measurements to the value of J_u. After measured asymmetries are published, more complex models may be used to determine J_u.

The spin-flip quark GPDs E_q in the factorized ansatz are given by [18]

$$E_\mathrm{q}(x,\xi,t) = \frac{E_\mathrm{q}(x,\xi)}{(1-t/0.71)^2}\,. \tag{10}$$

In the Regge ansatz the t-dependence is modeled in analogy to (9).

The t-independent part is parameterized using the double distribution ansatz

$$E_\mathrm{q}(x,\xi) = E_\mathrm{q}^{DD}(x,\xi) - \theta(\xi-|x|) D_\mathrm{q}\left(\frac{x}{\xi}\right)\,. \tag{11}$$

Note that the D-term has the same size but the opposite sign in (11) and (3). Therefore, it drops out when calculating J_q according to (1).

The double distribution has a form analogous to the spin-nonflip case:

$$E_\mathrm{q}^{DD}(x,\xi) = \int\limits_{-1}^{1} \mathrm{d}\beta \int\limits_{-1+|\beta|}^{1-|\beta|} \mathrm{d}\alpha\; \delta(x-\beta-\alpha\xi)\; K_\mathrm{q}(\beta,\alpha)\,, \tag{12}$$

with

$$K_\mathrm{q}(\beta,\alpha) = h(\beta,\alpha) e_\mathrm{q}(\beta)\,. \tag{13}$$

The spin-flip parton densities $e_\mathrm{q}(x)$ cannot be extracted from deep-inelastic scattering (DIS) data, unlike the case of spin-nonflip ones. Based on the chiral quark soliton model [18], the spin-flip density is taken as a sum of valence and sea quark contributions. Since in this model the sea part was found to be very narrowly peaked around $x=0$, the whole density is written as

$$e_\mathrm{q}(x) = A_\mathrm{q} q_\mathrm{val}(x) + B_\mathrm{q}\delta(x)\,. \tag{14}$$

In this expression, the shape of the valence quark part is given by that of the spin-nonflip density. The coefficients A_q and B_q are constrained by the total angular momentum sum rule (1) and the normalization condition

$$\int\limits_{-1}^{+1} \mathrm{d}x e_\mathrm{q}(x) = \kappa_\mathrm{q}\,, \tag{15}$$

where κ_q is the anomalous magnetic moment of quarks of flavor q ($\kappa_u = 2\kappa_\mathrm{p} + \kappa_n = 1.67$, $\kappa_d = \kappa_\mathrm{p} + 2\kappa_n = -2.03$). The constraints yield

$$A_\mathrm{q} = \frac{2\,J_\mathrm{q}^\mathrm{VGG} - M_\mathrm{q}^{(2)}}{M_{q_\mathrm{val}}^{(2)}}\,, \tag{16}$$

$$B_u = 2\left[\frac{1}{2}\kappa_u - \frac{2J_u^\mathrm{VGG} - M_u^{(2)}}{M_{u_\mathrm{val}}^{(2)}}\right]\,, \tag{17}$$

$$B_d = \kappa_d - \frac{2J_d^\mathrm{VGG} - M_d^{(2)}}{M_{d_\mathrm{val}}^{(2)}}\,. \tag{18}$$

The notation $J_\mathrm{q}^\mathrm{VGG}$ is used in order to emphasize the inherent model dependence of the parameterization. In (16)–(18), $M_\mathrm{q}^{(2)}$ and $M_{q_\mathrm{val}}^{(2)}$ are the parton momentum contributions to the proton momentum:

$$M_{q_\mathrm{val}}^{(2)} = \int\limits_0^1 x q_\mathrm{val}(x)\,\mathrm{d}x\,,$$

$$M_\mathrm{q}^{(2)} = \int\limits_0^1 x\left[q_\mathrm{val}(x) + 2\bar{q}(x)\right]\,\mathrm{d}x\,. \tag{19}$$

In the given scenario the total angular momenta carried by u- and d-quarks, J_u and J_d, enter directly as free parameters in the parameterization of the spin-flip GPD $E_\mathrm{q}(x,\xi,t)$. Hence the parameterization (14) can be used to investigate the sensitivity of hard electroproduction observables to variations in J_u^VGG and J_d^VGG.

As for the gluons, there exists no hint as to how the spin-flip GPD E_g could be described. There is an expectation that E_g will not be large compared to E_u and E_d [28]. Hence for simplicity throughout the present study E_g is neglected ("passive" gluons, i.e., $E_\mathrm{g}=0$).

As an example, Fig. 2 shows the t-independent part of various GPDs at $\xi = 0.1$, based on the MRST98 [29] parameterization of PDFs at $Q^2 = 4\,\mathrm{GeV}^2$. Using instead CTEQ6L PDFs [30] as input, the results for $u(d)$ quark GPDs are changed by less than 3% (10%); the GPD H_g

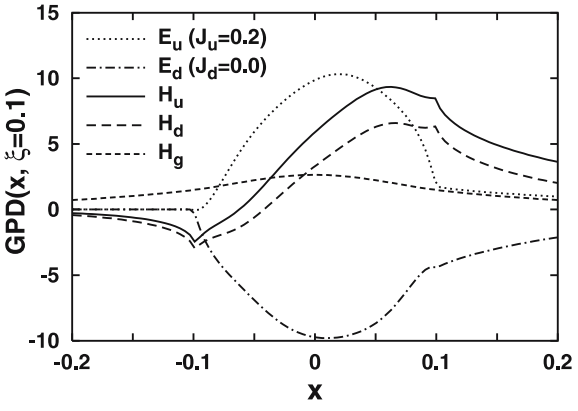

Fig. 2. t-independent part of quark and gluon GPDs at $Q^2 = 4\,\mathrm{GeV}^2$, $\xi = 0.1$ (MRST98 PDFs are used)

is up to 40% larger at $x = 0$. Because of u-quark dominance in electroproduction, uncertainties originating from d-quark PDFs can be safely neglected. Since gluons are absent in leading-order DVCS, uncertainties resulting from gluon PDFs have little influence on DVCS asymmetries and have been found to lead to a fractional change of up to 15% for the ρ^0 asymmetries. For the following calculations the MRST98 PDF set is taken.

3 Sensitivity of DVCS to the u-quark total angular momentum

3.1 Cross section and asymmetries

The fivefold cross section for the process $e(k)+p(p_1)\to e(k')+p(p_2)+\gamma(q_2)$ is given by

$$\frac{\mathrm{d}\sigma}{\mathrm{d}x_B\,\mathrm{d}y\,\mathrm{d}t\,\mathrm{d}\phi d\phi_S} = \frac{\alpha_{em}^3 x_B y}{16\pi^2 Q^2\sqrt{1+4x_B^2m^2/Q^2}}\cdot\left|\frac{\mathcal{T}}{e^3}\right|^2, \tag{20}$$

where $Q^2 = -q_1^2$ is the negative squared four-momentum of the virtual photon, $x_B = Q^2/(2p_1\cdot q_1)$ is the Bjorken variable, $t = (p_1 - p_2)^2$, $y = (p_1\cdot q_1)/(p_1\cdot k)$, $\mathcal{T}$ denotes the photon production amplitude, and e is the electron charge. Since the DVCS and Bethe–Heitler (BH) processes have an identical final state in which the photon is radiated either from a parton or from a lepton, respectively, $\mathcal{T}$ is given by the coherent sum of the BH amplitude $\mathcal{T}_{\mathrm{BH}}$ and the DVCS amplitude $\mathcal{T}_{\mathrm{DVCS}}$:

$$|\mathcal{T}|^2 = |\mathcal{T}_{\mathrm{BH}} + \mathcal{T}_{\mathrm{DVCS}}|^2 = |\mathcal{T}_{\mathrm{BH}}|^2 + |\mathcal{T}_{\mathrm{DVCS}}|^2 + \mathcal{I}, \tag{21}$$

in which

$$\mathcal{I} = \mathcal{T}_{\mathrm{BH}}^*\mathcal{T}_{\mathrm{DVCS}} + \mathcal{T}_{\mathrm{BH}}\mathcal{T}_{\mathrm{DVCS}}^* \tag{22}$$

describes the interference between both processes.

The coordinate system is defined in the target rest frame, as explained in Fig. 3. The theoretical formulae used below refer to the target being transversely polarized w.r.t. the virtual photon direction, while in the experiment the target polarization is transverse w.r.t. the incident lepton direction. At HERMES kinematics, these two directions are approximately parallel and the small longitudinal component ($< 10\%$) of the target polarization along the virtual photon direction is neglected in this study. Thus the reasonable approximation

$$\mathrm{d}\sigma = \mathrm{d}\sigma_{\mathrm{unp}} + \mathrm{d}\sigma_{\mathrm{TP}} \tag{23}$$

is used, where $\mathrm{d}\sigma_{\mathrm{unp}}$ ($\mathrm{d}\sigma_{\mathrm{TP}}$) denotes the cross section for the unpolarized (transversely polarized) component.

Since in the kinematic region of the HERMES experiment the DVCS cross section is typically much smaller than the BH cross section [32], the contribution of the DVCS term to the total cross section is neglected in what follows. The contributions of the BH term for an unpolarized beam are

$$\begin{aligned}\left|\mathcal{T}_{\mathrm{unp}}^{\mathrm{BH}}\right|^2 &= \frac{e^6}{x_B^2y^2(1+4x_B^2m^2/Q^2)^2tP_1(\phi)P_2(\phi)}\\ &\quad\times\left[c_{0,\mathrm{unp}}^{\mathrm{BH}} + c_{1,\mathrm{unp}}^{\mathrm{BH}}\cos\phi + c_{2,\mathrm{unp}}^{\mathrm{BH}}\cos 2\phi\right],\\ \left|\mathcal{T}_{\mathrm{TP}}^{\mathrm{BH}}\right|^2 &= 0\,.\end{aligned} \tag{24}$$

The full expressions for the BH propagators $P_1(\phi)$ and $P_2(\phi)$ and for the Fourier coefficients $c_{i,\mathrm{unp}}^{\mathrm{BH}}$ can be found in [33].[2]

The leading-twist and leading-order α_{s} contributions of the DVCS–BH interference term to the total cross section can be written as

$$\begin{aligned}\mathcal{I}_{\mathrm{unp}} &= \frac{\pm e^6}{x_By^3tP_1(\phi)P_2(\phi)}\left(c_{0,\mathrm{unp}}^{I} + c_{1,\mathrm{unp}}^{I}\cos\phi\right),\\ \mathcal{I}_{\mathrm{TP}} &= \frac{\pm e^6}{x_B^2y^2tP_1(\phi)P_2(\phi)}f\left(x_B,y,Q^2\right)\\ &\quad\times\left[\mathrm{Im}\widehat{M}_N\sin\left(\phi-\phi_S\right)\cos\phi + \mathrm{Im}\widehat{M}_S\cos\left(\phi-\phi_S\right)\sin\phi\right].\end{aligned} \tag{25}$$

Here $+(-)$ stands for a negatively (positively) charged lepton beam and $f\left(x_B,y,Q^2\right)$ is a kinematic prefactor independent of azimuthal angles. The full expressions for $c_{i,\mathrm{unp}}^{I}$ can be found in (53)–(56) of [33]. $\widehat{M}_N$ and $\widehat{M}_S$ are certain linear combinations of the Compton form factors $\mathcal{H}$, $\mathcal{E}$, $\widetilde{\mathcal{H}}$, and $\widetilde{\mathcal{E}}$, which are convolutions of the respective twist-2 GPDs H, E, $\widetilde{H}$, and $\widetilde{E}$ with the hard-scattering kernels as defined in (9) of [33].

The full expressions for $\widehat{M}_N$ and $\widehat{M}_S$ can be found in (71) in [33][2] or in (60) in [34]. Since $\xi \simeq x_B/(2-x_B)$ is small in a wide range of experimentally relevant kinematics, terms with prefactor ξ or x_B can be neglected, except

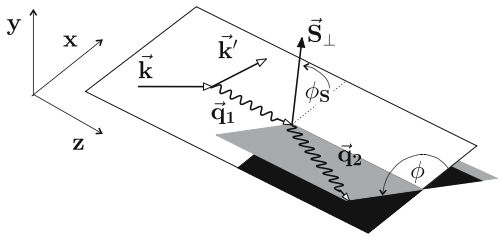

Fig. 3. Kinematics and azimuthal angles of photon electroproduction in target rest frame. The z-direction is chosen along the three-momenta of the virtual photon $\mathbf{q}_1$. The lepton three-momenta $\mathbf{k}$ and $\mathbf{k}'$ form the lepton scattering plane, while the three-momenta of virtual and real photons $\mathbf{q}_1$ and $\mathbf{q}_2$ define the production plane. The azimuthal angle of the production plane with respect to the scattering plane, around the virtual photon direction, is denoted as ϕ. Correspondingly, ϕ_S denotes the azimuthal angle of the target polarization vector with respect to the lepton scattering plane. In this frame the target polarization vector is given as $\mathbf{S}_\perp = (\cos\phi_S, \sin\phi_S, 0)$. The definitions conform with the Trento conventions [31]

[2] The azimuthal angles defined in this work are different from those used in [33]: $\phi = \pi - \phi_{[33]}$ and $\phi - \phi_S = \pi + \varphi_{[33]}$.

for the GPD $\widetilde{E}$ because the pion pole contribution to $\widetilde{E}$ scales like ξ^{-1}, so that $\widehat{M}_N$ and $\widehat{M}_S$ can be approximated as

$$\widehat{M}_N \simeq -\frac{t}{4M^2}\cdot\left[F_2\mathcal{H}-F_1\mathcal{E}\right],$$
$$\widehat{M}_S \simeq -\frac{t}{4M^2}\cdot\left[F_2\widetilde{\mathcal{H}}-F_1\xi\widetilde{\mathcal{E}}\right]. \quad (26)$$

Here F_1 and F_2 are the Dirac and Pauli form factors of the proton, respectively.

To constrain the GPDs involved in (26), the transverse polarization component of the interference term, $\mathcal{I}_{\mathrm{TP}}$, has to be singled out. This can be accomplished by forming the transverse (T) target-spin asymmetry with unpolarized (U) beam:

$$A_{\mathrm{UT}}(\phi,\phi_S) = \frac{\mathrm{d}\sigma(\phi,\phi_S)-\mathrm{d}\sigma(\phi,\phi_S+\pi)}{\mathrm{d}\sigma(\phi,\phi_S)+\mathrm{d}\sigma(\phi,\phi_S+\pi)} \quad (27)$$
$$\simeq A_{\mathrm{UT}}^{\sin(\phi-\phi_S)\cos\phi}\cdot\sin(\phi-\phi_S)\cos\phi + A_{\mathrm{UT}}^{\cos(\phi-\phi_S)\sin\phi}\cdot\cos(\phi-\phi_S)\sin\phi\,. \quad (28)$$

As $\left|\mathcal{T}_{\mathrm{unp}}^{\mathrm{BH}}\right|^2$ and $\mathcal{I}_{\mathrm{unp}}$ are independent of ϕ–ϕ_S, they do not appear in the numerators of (27). Since their dominant contribution to the denominator in (27) is given by $c_{0,\mathrm{unp}}^{\mathrm{BH}}$, the two amplitudes of the TTSA, $A_{\mathrm{UT}}^{\sin(\phi-\phi_S)\cos\phi}$ and $A_{\mathrm{UT}}^{\cos(\phi-\phi_S)\sin\phi}$, can be approximated as

$$A_{\mathrm{UT}}^{\sin(\phi-\phi_S)\cos\phi} \simeq \pm f\left(x_B,y,Q^2\right)\cdot\frac{\mathrm{Im}\widehat{M}_N}{c_{0,\mathrm{unp}}^{\mathrm{BH}}},$$
$$A_{\mathrm{UT}}^{\cos(\phi-\phi_S)\sin\phi} \simeq \pm f\left(x_B,y,Q^2\right)\cdot\frac{\mathrm{Im}\widehat{M}_S}{c_{0,\mathrm{unp}}^{\mathrm{BH}}}. \quad (29)$$

Note that the approximations used in this section are for illustrative purposes only and are not used in the numerical calculations described below.

3.2 Expected value of TTSA and projected statistical uncertainty

Since in the DVCS process the gluons enter only in NLO in α_S, their contributions to the cross section and TTSA are neglected. For the quarks, it can be seen from (26) that, besides the GPDs H and E that were discussed in Sect. 2, there are two other GPDs, $\widetilde{H}$ and $\widetilde{E}$, involved in the TTSA for DVCS. As they are not the main interest of this paper, in the calculations below they are always included and kept unchanged. In their model description, the forward limit of the GPD $\widetilde{H}$ is fixed by the quark helicity distributions $\Delta q(x,\mu^2)$, while the GPD $\widetilde{E}$ is evaluated from the pion pole, which only provides a real part to $\widehat{M}_S$ in (26).

At present, there exists a code (M. Vanderhaeghen, pers. commun.)designed to calculate observables in the exclusive reaction $ep\to ep\gamma$. It has been used (see appendix) to evaluate the TTSA arising from the DVCS–BH interference. The TTSA is calculated for the case of positive beam charge, at the average kinematic values per bin in x_B, Q^2, and t taken from a measurement of the beam-spin asymmetry in DVCS at HERMES [24] (see Table 1).

The statistical error of an asymmetry is independent of its size if the asymmetry itself is small. For a beam (target) single-spin asymmetry it is obtained as

$$\sigma_{stat}^2 \propto \frac{1}{N}\cdot\frac{1}{P_{\mathrm{beam(target)}}^2}, \quad (30)$$

where N is the total number of events that is proportional to the integrated luminosity and $P_{\mathrm{beam(target)}}$ is the beam (target) polarization. The following projection is based on a HERMES data set of 8 million DIS events to be taken with an unpolarized positron beam and a transversely polarized hydrogen target. Using the known statistical errors of the beam-spin asymmetry measurement at HERMES on an unpolarized hydrogen target (7 million DIS events, $P_{\mathrm{beam}}\simeq 50\%$) [24], the projected statistical error for the TTSA is obtained.

Table 1. Average kinematic values for Q^2, x_B, and $-t$ bins and statistical errors, taken from a measurement of the beam-spin asymmetry at HERMES [24]

Q^2 bin (GeV^2)	1.00–1.50	1.50–2.30	2.30–3.50	3.50–6.00	6.00–10.0
$\langle Q^2\rangle$ (GeV^2)	1.2	1.8	2.8	4.4	7.1
$\langle x_B\rangle$	0.06	0.08	0.10	0.15	0.24
$\langle -t\rangle$ (GeV^2)	0.07	0.09	0.12	0.17	0.24
stat. $\delta A_{\mathrm{LU}}^{\sin\phi}$	0.053	0.050	0.061	0.070	0.163
x_B bin	0.03–0.07	0.07–0.10	0.10–0.15	0.15–0.20	0.20–0.35
$\langle Q^2\rangle$ (GeV^2)	1.4	2.2	3.1	4.5	6.1
$\langle x_B\rangle$	0.05	0.08	0.12	0.17	0.24
$\langle -t\rangle$ (GeV^2)	0.08	0.10	0.12	0.17	0.22
stat. $\delta A_{\mathrm{LU}}^{\sin\phi}$	0.048	0.053	0.060	0.099	0.145
$-t$ bin (GeV^2)	0.00–0.06	0.06–0.14	0.14–0.30	0.30–0.50	0.50–0.70
$\langle Q^2\rangle$ (GeV^2)	2.0	2.5	3.0	3.6	3.9
$\langle x_B\rangle$	0.08	0.10	0.11	0.12	0.12
$\langle -t\rangle$ (GeV^2)	0.03	0.09	0.20	0.37	0.57
stat. $\delta A_{\mathrm{LU}}^{\sin\phi}$	0.041	0.052	0.066	0.126	0.263

The projections for $A_{\mathrm{UT}}^{\sin(\phi-\phi_S)\cos\phi}$ and $A_{\mathrm{UT}}^{\cos(\phi-\phi_S)\sin\phi}$ are calculated for different values of the total angular momentum J_u^{VGG}. Since the contributions of u-quark and d-quark are proportional to the corresponding squared charge, the d-quark contribution is suppressed, and hence in the calculations a fixed value is used for J_d^{VGG}. The latter was chosen to be $J_d^{\mathrm{VGG}} = 0$, inspired by the results of recent lattice calculations (see, e.g., [35]). Using both Regge and factorized ansätze, the asymmetries are calculated for the four possible cases setting the profile parameters b_{val} and b_{sea} to either one or infinity. Comparing all sets of projections to each other, the amplitudes of the TTSA appear to be sensitive only to the change in b_{sea} from one to infinity. The corresponding differences are small and can be seen by comparing Figs. 4 and 5, where the amplitudes are shown in dependence on Q^2, x_B, and $-t$ together with the projected statistical errors. To study the contributions of the GPDs H, $\widetilde{H}$, and $\widetilde{E}$ alone, calculations are done for $E = 0$ as well.

As expected from (26) and (29), variations in the parameter settings for the GPD E become manifest in $A_{\mathrm{UT}}^{\sin(\phi-\phi_S)\cos\phi}$ while $A_{\mathrm{UT}}^{\cos(\phi-\phi_S)\sin\phi}$ shows only minor changes. The latter are apparent only in the kinematic regime of large x_B or correspondingly large Q^2 since the contribution of the GPDs E_{q} to $\widehat{M}_S$ is suppressed by x_B and thus has been neglected in (26). Within these model calculations $A_{\mathrm{UT}}^{\sin(\phi-\phi_S)\cos\phi}$ turns out to be sizable even when the calculation is done for $E_{\mathrm{q}} = 0$. Thus a solid knowledge of the GPD H_u is needed in order to constrain J_u^{VGG}. It has been shown [36] that the model parameters for the GPD H_u, in particular the size of the profile parameters b_{val} and b_{sea}, can be well constrained by the envisaged HERMES DVCS measurements until 2007, using an unpolarized hydrogen target. Since in addition the profile parameters are assumed to be the same for the GPD E_u, the only remaining free parameter is J_u^{VGG}. Hence the projected measurement of $A_{\mathrm{UT}}^{\sin(\phi-\phi_S)\cos\phi}$ has a clear potential to constrain J_u^{VGG}, as can be seen from the left panels of Figs. 4 and 5.

The discriminative power of the envisaged TTSA measurement can be enhanced by combining all data into one point, since all considered models show the same kinematic dependences. The corresponding statistical power of a HERMES data set based on 8 million DIS events is shown in Fig. 6, for b_{sea} equal to one or infinity, and for three different values of the total u-quark angular momentum J_u^{VGG} plus the special case $E_{\mathrm{q}} = 0$.

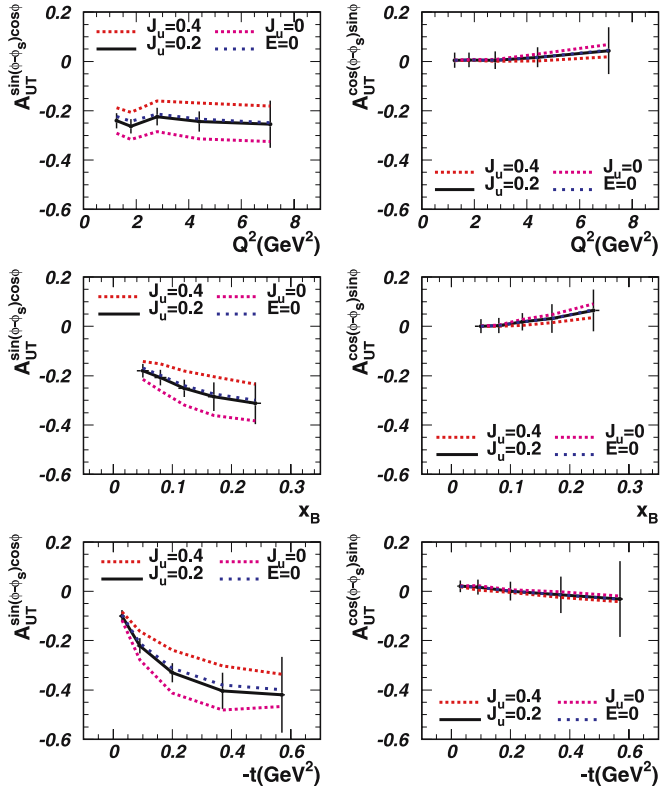

Fig. 4. Expected DVCS TTSA amplitudes $A_{UT}^{\sin(\phi-\phi_S)\cos\phi}$ and $A_{UT}^{\cos(\phi-\phi_S)\sin\phi}$ in Regge ansatz for $b_{\mathrm{val}} = 1$, $b_{\mathrm{sea}} = \infty$, $J_u^{\mathrm{VGG}} = 0.4$ $(0.2, 0)$, $J_d^{\mathrm{VGG}} = 0$. $E = 0$ denotes zero effective contribution from the quark GPDs E_{q}. The calculations are done at the average kinematic values as listed in Table 1. Projected statistical errors are shown

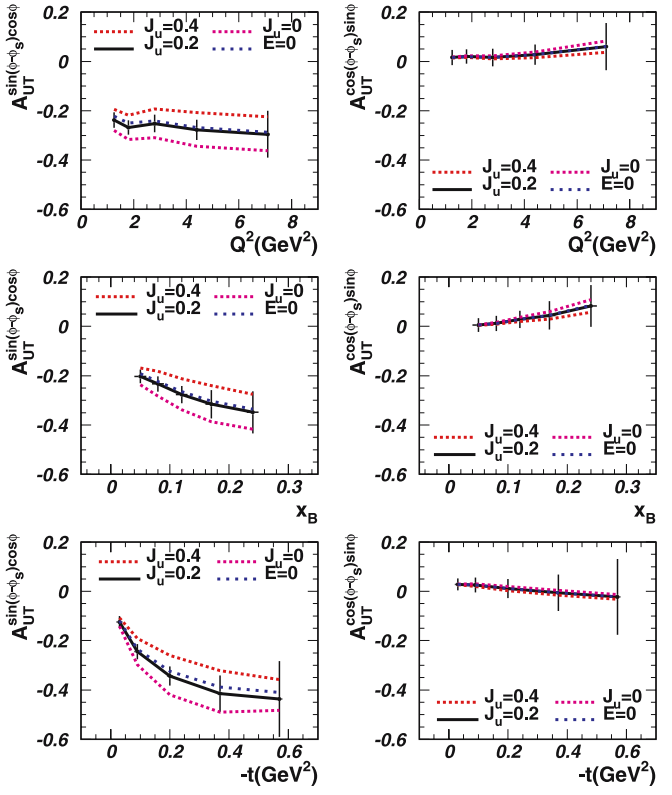

Fig. 5. Expected DVCS TTSA amplitudes $A_{UT}^{\sin(\phi-\phi_S)\cos\phi}$ and $A_{UT}^{\cos(\phi-\phi_S)\sin\phi}$ in Regge ansatz for $b_{\mathrm{val}} = 1$, $b_{\mathrm{sea}} = 1$, $J_u^{\mathrm{VGG}} = 0.4$ $(0.2, 0)$, $J_d^{\mathrm{VGG}} = 0$. $E = 0$ denotes zero effective contribution from the quark GPDs E_{q}. The calculations are done at the average kinematic values as listed in Table 1. Projected statistical errors are shown

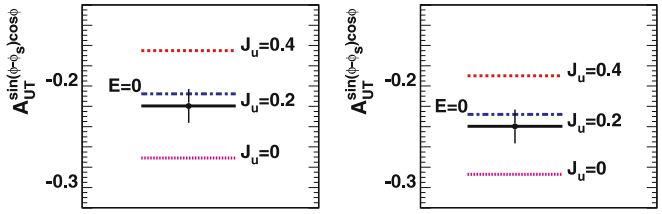

Fig. 6. Expected DVCS TTSA amplitudes $A_{\mathrm{UT}}^{\sin(\phi-\phi_S)\cos\phi}$ with $b_{\mathrm{val}}=1$ and $b_{\mathrm{sea}}=\infty$ (*left panel*) or $b_{\mathrm{sea}}=1$ (*right panel*), $J_u^{\mathrm{VGG}}=0.4\,(0.2,0)$, $J_d^{\mathrm{VGG}}=0$ in Regge ansatz at average kinematics of full measurement. $E=0$ denotes zero effective contribution from GPDs E_{q}. The projected statistical error for 8 million DIS events is shown. The systematic error is expected not to exceed the statistical one

It appears that for $b_{\mathrm{sea}}=1$ ($b_{\mathrm{sea}}=\infty$) the amplitude ranges between values of -0.17 and -0.27 (-0.19 and -0.29) when J_u^{VGG} ranges between 0 and 0.4. The projected statistical error for these integrated TTSA amplitudes is 0.017. Extrapolating the knowledge of the systematic uncertainty from the analysis of 2000 HERMES data [24], its size can be expected to not exceed the statistical error, such that a total experimental uncertainty below 0.025 appears to be a realistic estimate. Altogether, the difference in the size of the TTSA due to a change in J_u^{VGG} between 0 and 0.4 corresponds to a 4σ effect, where σ denotes the total experimental uncertainty. Thus, based on the GPD model used it can be expected that the upcoming DVCS results from HERMES will provide a constraint on the size of J_u^{VGG}.[3]

4 Sensitivity of elastic ρ^0 electroproduction to the u-quark total angular momentum

Also, a measurement of the TTSA in elastic vector meson electroproduction can be a source of information about the spin-flip generalized parton distribution E. An estimate for the asymmetry was obtained in [18] using the factorized model of GPDs described in Sect. 2 without inclusion of gluons. The scope of this section is to additionally include the Regge ansatz to check the assumption that the gluon contribution to the ρ^0 electroproduction cross section is small and to eventually calculate the size of the TTSA at HERMES kinematics. The issue is raised since, in contrast to DVCS, in vector meson elastic electroproduction gluons enter at the same order of α_{s} as quarks, namely at order α_{s} to the power one. Hence this channel appears as one of the rare cases where gluon GPDs may be accessed through HERMES data.

[3] The recent switch of the HERA accelerator to an electron beam will also require doing the above calculations for the negative beam charge. However, the sensitivity to J_u^{VGG} of the combined electron and positron measurements is expected to be similar to that calculated here for a positron beam only.

4.1 Cross section and gluonic contribution

It was shown [37] that the leading-twist contribution to exclusive electroproduction of vector mesons requires that both the virtual photon and the vector meson be longitudinal, i.e., transversely polarized. Therefore the present calculations cover only the longitudinal part of the cross section. The $\gamma_{\mathrm{L}}^* p\to\rho^0 p'$ cross section is given by [18]

$$\frac{\mathrm{d}\sigma_{\mathrm{L}}}{\mathrm{d}t}=\frac{1}{8m\pi(W^2-m^2)|\mathbf{q}_1|}\Big(|\mathcal{T}_A|^2+|\mathcal{T}_B|^2\Big)\,, \tag{31}$$

where $\mathbf{q}_1$ is the momentum of the virtual photon in the center of mass system of this photon and the initial proton, while W is their invariant mass. The spin-flip amplitude reads

$$\begin{aligned}\mathcal{T}_A&=-\mathrm{i}e\frac{2\sqrt{2}\pi\alpha_{\mathrm{s}}}{9Q}\mathcal{A}\bar{u}(p_2)n^\mu\gamma_\mu u(p_1)\int\limits_0^1\mathrm{d}z\frac{\Phi(z)}{z} \\ &\simeq-\mathrm{i}\mathcal{A}\pi e\alpha_{\mathrm{s}}\frac{8}{9}\frac{1}{Q}\int\limits_0^1\mathrm{d}z\frac{\Phi(z)}{z}\,,\end{aligned} \tag{32}$$

and the spin-nonflip one is[4]

$$\begin{aligned}\mathcal{T}_B&=e\frac{\sqrt{2}\pi\alpha_{\mathrm{s}}}{9Qm}\mathcal{B}\bar{u}(p_2)\sigma^{\mu\nu}n_\mu\Delta_\nu u(p_1)\int\limits_0^1\mathrm{d}z\frac{\Phi(z)}{z} \\ &\simeq-\mathrm{i}\mathcal{B}\pi e\alpha_{\mathrm{s}}\frac{|\Delta_T|}{m}\frac{4}{9}\frac{1}{Q}\int\limits_0^1\mathrm{d}z\frac{\Phi(z)}{z}\,.\end{aligned} \tag{33}$$

Here $n=(1,0,0,-1)/(\sqrt{2}(p_1+p_2)^+)$ is a lightlike vector along the z-axis and $\Delta=p_2-p_1$ is the four-momentum transfer ($\Delta^2=t$) whose transverse component modulus is given by $|\Delta_T|=\sqrt{-t(1-\xi^2)-4\xi^2m^2}$. The ρ^0-meson wave function is taken in the form

$$\Phi(z)=6z(1-z)f_\rho\,, \tag{34}$$

with $f_\rho=0.216\,\mathrm{GeV}$ and z being the meson longitudinal momentum fraction carried by a parton. The complex factors $\mathcal{A}$ and $\mathcal{B}$ are given by

$$\begin{aligned}\mathcal{A}=\frac{1}{\sqrt{2}}\int\limits_{-1}^1\Big(&e_uH_u(x,\xi,t)-e_dH_d(x,\xi,t) \\ &+\frac{3}{8}(e_u-e_d)\frac{H_{\mathrm{g}}(x,\xi,t)}{x}\Big) \\ &\times\Big\{\frac{1}{x-\xi+\mathrm{i}\epsilon}+\frac{1}{x+\xi-\mathrm{i}\epsilon}\Big\}\mathrm{d}x\,,\end{aligned} \tag{35}$$

[4] In the subsequent calculations the exact formulae were used.

$$\mathcal{B} = \frac{1}{\sqrt{2}} \int_{-1}^{1} \Big(e_u E_u(x,\xi,t) - e_d E_d(x,\xi,t) + \frac{3}{8}(e_u - e_d)\frac{E_{\rm g}(x,\xi,t)}{x} \Big) \times \Big\{ \frac{1}{x-\xi+{\rm i}\epsilon} + \frac{1}{x+\xi-{\rm i}\epsilon} \Big\} {\rm d}x \,. \quad (36)$$

The TTSA is defined as

$$A_{\rm UT}(\phi-\phi_S) = \frac{{\rm d}\sigma(\phi-\phi_S) - {\rm d}\sigma(\phi-\phi_S+\pi)}{{\rm d}\sigma(\phi-\phi_S) + {\rm d}\sigma(\phi-\phi_S+\pi)} = A_{\rm UT}^{\sin(\phi-\phi_S)} \cdot \sin(\phi-\phi_S) \,. \quad (37)$$

The $A_{\rm UT}^{\sin(\phi-\phi_S)}$ amplitude of the TTSA can be expressed in terms of the spin-flip and spin-nonflip amplitudes as [18]

$$A_{\rm UT}^{\sin(\phi-\phi_S)} = \frac{{\rm Im}(\mathcal{A}\mathcal{B}^*)|\Delta_T|/m}{(1-\xi^2)|\mathcal{A}|^2 - (\xi^2 + \frac{t}{4m^2})|\mathcal{B}|^2 - 2\xi^2 {\rm Re}(\mathcal{A}\mathcal{B}^*)} \,. \quad (38)$$

Note that, because the Trento convention [31] is used, the sign of this equation is opposite to that in [18] and the normalization is larger by a factor of $\pi/2$.

The cross section is calculated using both factorized and Regge ansätze for GPDs.[5] The value $b = 1$ is taken for the profile parameter both for sea and valence quarks. It is found that using $b_{\rm sea} = \infty$ instead of $b_{\rm sea} = 1$ leads to a rise of the cross section by a factor of about 1.15. The value $b_{\rm val} = b_{\rm sea} = 1$ is chosen to provide a direct comparison to previous calculations [18, 38]. The value of the profile parameter for gluons is chosen as $b = 2$, and it has been checked that choosing $b = 1$ or ∞ does not change the cross section by more than 20%. The W-dependence of the cross section for $Q^2 = 4\,{\rm GeV}^2$ is shown in Fig. 7. For both ansätze the calculations overshoot considerably the experimental data from HERMES [39]. However, a significant reduction in the calculated cross section might be expected if transverse motion effects are taken into account [18, 38]. On the other hand, also the double-distribution-based calculations of the DVCS cross section have been found to overshoot the data from H1 [40, 41].

An unexpected result of the calculation shown in Fig. 7 is a quite small (15%–20%) pure quark contribution to the cross section, while in [18, 38] the quark contribution was found to be dominant. Comparing the calculated quark contribution to experimental data (also shown in Fig. 7), it could also be concluded that the gluon contribution in the present calculation is substantially overestimated, while the quark contribution itself is reasonable and can explain alone (in the factorized ansatz) the value of the measured cross section. However, there exists experimental evidence that the gluon spin-nonflip part is indeed large [28].

[5] The principal values of the integrals in (35) and (36) are calculated in the following way: $\int_{a<0}^{b>0} \frac{f(x)}{x}\,{\rm d}x = f(b)\ln(b) - f(a)\ln(a) - \int_{\rm a}^{0} f'(x)\ln(x)\,{\rm d}x + \int_{0}^{b} f'(x)\ln(x)\,{\rm d}x$. In this way the nonintegrable singularity is exchanged by an integrable one.

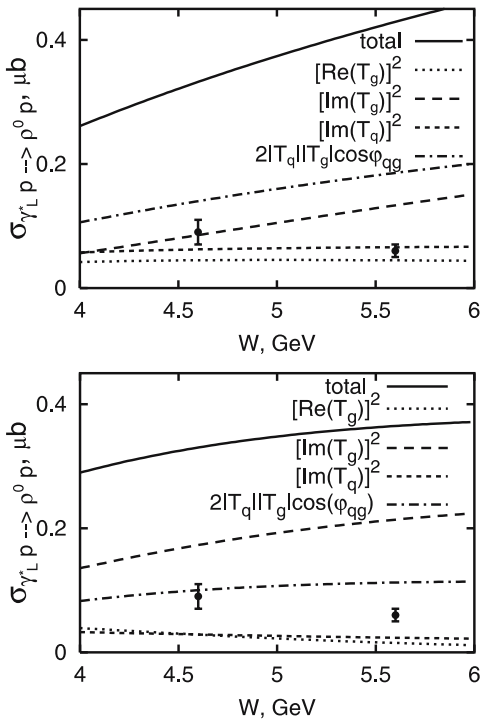

Fig. 7. Calculated W-dependence of hard exclusive ρ^0 electroproduction cross section at $Q^2 = 4\,{\rm GeV}^2$ for factorized (*top*) and Regge (*bottom*) GPD models compared to HERMES data [39]. $\mathcal{T}_{\rm q}$ and $\mathcal{T}_{\rm g}$ are the quark and gluon amplitudes, respectively. The quark real part is very small and is not shown

On the amplitude level, the cross sections of ρ^0 and ϕ mesons are given as

$$\sigma_{\rho^0} = C_{\rho^0}|\mathcal{T}_{\rm q} + \mathcal{T}_{\rm g}|^2 = C_{\rho^0}(|\mathcal{T}_{\rm q}|^2 + 2|\mathcal{T}_{\rm q}||\mathcal{T}_{\rm g}|\cos(\varphi_{\rm qg}) + |\mathcal{T}_{\rm g}|^2), \quad (39)$$
$$\sigma_\phi = \frac{2}{9} C_\phi |\mathcal{T}_{\rm g}|^2 \,.$$

Here $\mathcal{T}_{\rm q}$ is the quark amplitude, $\mathcal{T}_{\rm g}$ the gluon amplitude (the s-quark contribution to the ϕ production amplitude is neglected), and $\varphi_{\rm qg}$ the effective phase between the quark and gluon amplitudes. In the existing GPD-based calculations [18, 38], both quark and gluon contributions are dominated by the imaginary parts that have the same sign, i.e., $\varphi_{\rm qg} \simeq 0$. In the present model the calculation $\varphi_{\rm qg} \simeq 30^\circ$ is obtained. Considering the wave functions of ρ^0 and ϕ mesons to be similar (as is supported by the measured values of their decay widths), $C_{\rho^0} \simeq C_\phi$ follows, and the ratio of ϕ to ρ^0 cross sections reads

$$\frac{\sigma_\phi}{\sigma_{\rho^0}} = \frac{2}{9} \frac{|\mathcal{T}_{\rm g}|^2}{|\mathcal{T}_{\rm q}|^2 + 2|\mathcal{T}_{\rm q}||\mathcal{T}_{\rm g}|\cos(\varphi_{\rm qg}) + |\mathcal{T}_{\rm g}|^2} \,. \quad (40)$$

At HERMES, the ratio of $\sigma_\phi/\sigma_{\rho^0}$ was measured [43]. The experimental value was 0.08 ± 0.01, slightly increasing with Q^2. Inserting it into the left-hand side (l.h.s.) of (40) and taking $\varphi_{\rm qg} = 0^\circ$ (30°) yields $\left.\frac{|\mathcal{T}_{\rm q}|}{|\mathcal{T}_{\rm g}|}\right|_{\rm HERMES} = 0.7$ (0.78). This value is in good agreement with the results of

the present calculation, where $\frac{|\mathcal{T}_q|}{|\mathcal{T}_g|}$ ranges between 0.8 and 0.5 (0.5 and 0.3) for the factorized (Regge) ansatz when W increases from 4 to 6 GeV. This is in contrast to the above-mentioned result of a dominant quark contribution, $\frac{|\mathcal{T}_q|}{|\mathcal{T}_g|} \simeq 3$ [18,38]. Hence the gluon contribution H_g cannot be neglected. Thus, in order to arrive at the measured cross section, both quark and gluon amplitudes have to be scaled down in a similar proportion, leaving essentially unchanged the expected TTSA value that will be calculated in what follows.

4.2 Expected value of TTSA and projected statistical uncertainty

The $A_{UT}^{\sin(\phi-\phi_S)}$ amplitude of the TTSA in (38) is calculated at HERMES kinematics. The statistical error is extrapolated from a preliminary analysis of the HERMES longitudinal target-spin asymmetry measured on the deuteron [44] that is based on 8 million DIS events. In the latter analysis the data are not split into parts corresponding to longitudinal and transverse virtual photons, while the present calculation is related to longitudinal photons only. At HERMES kinematics ($\langle Q^2\rangle \simeq 2\,\mathrm{GeV}^2$), longitudinal photons constitute about 50% of all virtual photons. Also, the transverse target polarization is 0.75 while the longitudinal one is 0.85. The projected statistical error for 8 million DIS events taken on a transversely polarized target is hence larger by a factor $\sqrt{2}\frac{0.85}{0.75} = 1.6$ compared to that of [44]. Note that this error estimate may be considered "optimistic" since it assumes that the contribution to the asymmetry from longitudinal and transverse photons can be completely disentangled.

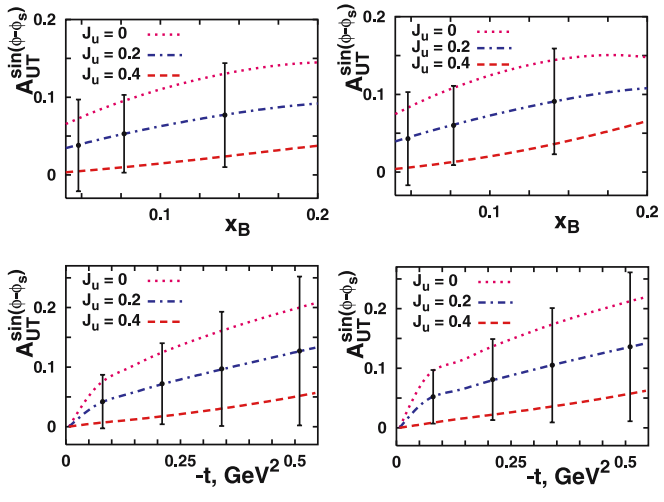

Fig. 8. Comparison of expected $A_{UT}^{\sin(\phi-\phi_s)}$ amplitudes of ρ^0 TTSAs calculated in Regge ansatz with $b_{val} = 1$ and $b_{sea} = 1$ (*left*) or $b_{sea} = \infty$ (*right*). Average kinematic values $\langle -t\rangle = 0.14\,\mathrm{GeV}^2$ and $\langle x_B\rangle = 0.085$ for x_B and t-dependences, respectively, and $\langle Q^2\rangle = 2\,\mathrm{GeV}^2$ correspond to a preliminary analysis of HERMES data on a longitudinally polarized deuterium target [44]. Projected statistical errors are shown. The systematic uncertainty is expected to be smaller than the statistical one

The calculated x_B- and t-dependences of $A_{UT}^{\sin(\phi-\phi_S)}$ are shown in Fig. 8 for different values of J_u^{VGG}. As in the case of DVCS, J_d^{VGG} is fixed inspired by the fact that the d-quark contribution is still suppressed, although the suppression in ρ^0 production is half as strong as in DVCS. Again, the choice of $J_d^{VGG} = 0$ is based on the results of recent lattice calculations (see, e.g., [35]). Note that in contrast to DVCS, $E = 0$ results in a vanishing asymmetry. As can be seen by comparing Fig. 8 to Figs. 4 and 5, the expected magnitude of $A_{UT}^{\sin(\phi-\phi_S)}$ in ρ^0 production is much smaller than in DVCS. This is due to a large gluonic contribution to the amplitude, which is considered "passive" ($E_g = 0$, $H_g \neq 0$), i.e., the gluons dilute the asymmetry in this case. It was found that the difference in $A_{UT}^{\sin(\phi-\phi_S)}$ between the factorized and Regge ansätze was negligible. Also, the variation of b_{sea} only leads to a small difference as can be seen when comparing the left and right panels of Fig. 8, where x_B- and t-dependences of the $A_{UT}^{\sin(\phi-\phi_S)}$ amplitude of the asymmetry are shown for $b_{sea} = 1$ and $b_{sea} = \infty$, respectively. The amplitude of the integrated TTSA is shown in Fig. 9, for the same two cases. It is essentially independent of b_{sea} and ranges between values of 0.10 and 0.01 when J_u^{VGG} ranges between 0 and 0.4.

The projected statistical error for the integrated TTSA amplitudes is 0.034. Extrapolating the knowledge on the systematic uncertainty from [44], its size can be expected to be about 0.02 such that a total experimental uncertainty below 0.04 appears as a realistic estimate. Altogether, the difference in $A_{UT}^{\sin(\phi-\phi_S)}$ due to a change of J_u^{VGG} between 0 and 0.4 corresponds to an approx. 2σ effect, where σ denotes the total experimental uncertainty. Thus it can be expected that the upcoming ρ^0 electroproduction measurements performed at HERMES will provide an additional constraint on the size of J_u^{VGG}.

A tempting possibility provided by ρ^0 production is related to an estimate of the gluonic content of E. Strongly simplifying, (38) represents the ratio $E/H \propto (E_q + E_g)/(H_q + H_g)$. Hence, when comparing the earlier calculations [18] where gluons have been neglected ($E_g = H_g = 0$) to the case of "passive" gluons presented above ($E_g = 0$, $H_g \neq 0$), the asymmetry gets smaller ("diluted") by the presence of the term containing H_g in the

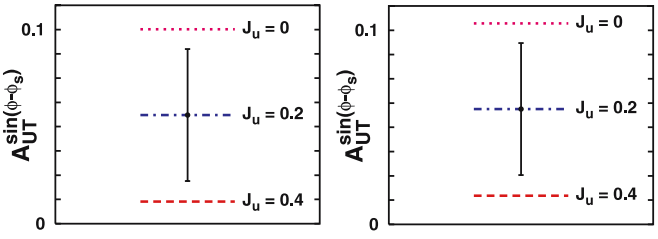

Fig. 9. Comparison of expected $A_{UT}^{\sin(\phi-\phi_s)}$ amplitudes of ρ^0 TTSAs calculated at average HERMES kinematics ($\langle -t\rangle = 0.14\,\mathrm{GeV}$, $\langle x_B\rangle = 0.085$, $\langle Q^2\rangle = 2\,\mathrm{GeV}$) in Regge ansatz with $b_{val} = 1$ and $b_{sea} = 1$ (*left*) or $b_{sea} = \infty$ (*right*). Projected statistical errors are shown. The systematic uncertainty is expected to be smaller than the statistical one

denominator. On the other hand, if the measured asymmetry is found to be large, this could imply that the gluons are "active" ($E_{\rm g} \neq 0$), so that their contribution to the spin-flip amplitude cannot be neglected.

5 Summary and outlook

Transverse target-spin asymmetries (TTSAs) in DVCS and ρ^0 elastic electroproduction are the only candidates known at present to access the GPD E on a proton target, in which E comes as a leading term.

In the present study, a code (M. Vanderhaeghen, pers. commun.)based on a model developed in [18, 38] is used to calculate the expected TTSAs to be measured in DVCS on the HERMES transversely polarized hydrogen target. To check the accessibility of E at HERMES, different parameterization ansätze and parameters of H and E are chosen. As the model for E depends on the total angular momentum of the u-quarks in the proton, the possibility arises of checking the sensitivity of the data to different values chosen as $J_u^{\rm VGG} = 0.4, 0.2, 0.0$, while on the basis of u-quark dominance and recent lattice calculations (see, e.g., [35]) a fixed-value $J_d^{\rm VGG} = 0$ is used. The calculations are performed at the HERMES average kinematic values [24]. The results show that the DVCS TTSA amplitude $A_{\rm UT}^{\sin(\phi-\phi_S)\cos\phi}$ is sensitive to the GPD E and thus to the total u-quark angular momentum $J_u^{\rm VGG}$, while $A_{\rm UT}^{\cos(\phi-\phi_S)\sin\phi}$ is not. It was found that, aside from $J_u^{\rm VGG}$, the amplitude $A_{\rm UT}^{\sin(\phi-\phi_S)\cos\phi}$ is largely independent of different parameterization ansätze and model parameters. Projected statistical errors for the asymmetries are evaluated by converting those from [24] to a data set corresponding to 8 million DIS events taken on a transversely polarized hydrogen target.

The same parameterizations are used to calculate the TTSA in ρ^0 electroproduction by longitudinal virtual photons. The main difference to the DVCS case is a large gluonic contribution to the amplitude. At present, only the spin-nonflip part of the gluonic amplitude can be reasonably described, while the spin-flip gluonic GPD $E_{\rm g}$ is totally unknown. Therefore, throughout the calculation $E_{\rm g}$ is set to zero ("passive" gluons). Under this assumption, the situation in ρ^0 electroproduction appears less favorable concerning the sensitivity of the expected TTSA amplitude to the total angular momentum $J_u^{\rm VGG}$. However, should the value of the amplitude be measured larger than that predicted by these calculations, this would imply that $E_{\rm g}$ cannot be neglected and thus indicate that gluons inside the proton carry significant orbital angular momentum.

Altogether, transverse target-spin asymmetries in both DVCS and ρ^0 electroproduction are studied, in the context of a model for the GPDs H and E, to evaluate projected uncertainties for extracting the value of J_u from future data. Considering all anticipated HERMES data to be taken for DVCS (ρ^0-production), the projected total experimental 1σ-uncertainty is estimated to correspond to a range of about 0.1 (0.2) in J_u.

Acknowledgements. This study would have been impossible without the constant advice of M. Diehl. The support of J. Volmer is highly appreciated by Z.Y., and A.V. is grateful to A. Borissov for useful discussions. The advice of E. Aschenauer is appreciated. A.V. was supported by the Alexander von Humboldt foundation, RFBR Grants 04-02-16445, 03-02-17291 and the Heisenberg–Andau program. This work was supported in part by the US Department of Energy.

Appendix : TTSA Calculation in DVCS

A code (M. Vanderhaeghen, pers. commun.)is used to estimate the TTSA related to DVCS. The coordinate system and angles defined in the code are the same as depicted in Fig. 3. The polarization of the target in the code is defined according to the virtual photon direction. For a transversely polarized target, the target polarization direction can be chosen either in the lepton plane (x-direction) or perpendicular to it (y-direction). The former corresponds to $\phi_S = 0$ or π, the latter to $\phi_S = \pi/2$ or $3\pi/2$. Therefore, the following intermediate asymmetries can be calculated:

$$A_x(\phi) = \frac{{\rm d}\sigma_{\phi_S=0}(\phi) - {\rm d}\sigma_{\phi_S=\pi}(\phi)}{{\rm d}\sigma_{\phi_S=0}(\phi) + {\rm d}\sigma_{\phi_S=\pi}(\phi)},$$
$$A_y(\phi) = \frac{{\rm d}\sigma_{\phi_S=\frac{\pi}{2}}(\phi) - {\rm d}\sigma_{\phi_S=\frac{3\pi}{2}}(\phi)}{{\rm d}\sigma_{\phi_S=\frac{\pi}{2}}(\phi) + {\rm d}\sigma_{\phi_S=\frac{3\pi}{2}}(\phi)}. \qquad \text{(A.1)}$$

Defining the following functions

$$A_1(\phi) = A_x \cdot \sin\phi - A_y \cdot \cos\phi, \qquad \text{(A.2)}$$
$$A_2(\phi) = A_x \cdot \cos\phi + A_y \cdot \sin\phi,$$

the contribution of the transverse target polarization component of the interference term $\mathcal{I}_{\rm TP}$ to the total cross section in (25) can be expressed as

$${\rm d}\sigma_{\rm TP} = {\rm d}\sigma_{\rm unp}\Big[A_1(\phi)\cdot\sin(\phi-\phi_S) + A_2(\phi)\cdot\cos(\phi-\phi_S)\Big]. \qquad \text{(A.3)}$$

Therefore, the asymmetries defined in (28) can be computed as

$$A_{\rm UT}^{\sin(\phi-\phi_S)\cos\phi} = A_1^{\cos\phi},$$
$$A_{\rm UT}^{\cos(\phi-\phi_S)\sin\phi} = A_2^{\sin\phi}. \qquad \text{(A.4)}$$

References

1. F.M. Dittes et al., Phys. Lett. B **209**, 325 (1988)
2. D. Müller et al., Fortschr. Phys. **42**, 101 (1994)
3. X.D. Ji, Phys. Rev. D **55**, 7114 (1997)
4. A.V. Radyushkin, Phys. Lett. B **385**, 333 (1996)
5. A.V. Radyushkin, Phys. Rev. D **56**, 5524 (1997)
6. X.D. Ji, Phys. Rev. Lett. **78**, 610 (1997)
7. M. Diehl, Phys. Rep. **388**, 41 (2003)

8. A.V. Belitsky, A. Freund, D. Müller, Nucl. Phys. B **574**, 347 (2000)
9. M. Burkardt, Phys. Rev. D **62**, 071 503 (2000) [Erratum-ibid. D **66**, 119 903 (2002)]
10. J.P. Ralston, B. Pire, Phys. Rev. D **66**, 111 501 (2002)
11. M. Diehl, Eur. Phys. J. C **25**, 223 (2002) [Erratum-ibid. C **31**, 277 (2003)]
12. M. Burkardt, Int. J. Mod. Phys. A **18**, 173 (2003)
13. H1 Collaboration, C. Adloff et al., Phys. Lett. B **517**, 47 (2001)
14. ZEUS Collaboration, S. Chekanov et al., Phys. Lett. B **573**, 46 (2003)
15. HERMES Collaboration, F. Ellinghaus, Nucl. Phys. A **711**, 171 (2002)
16. HERMES Collaboration, A. Airapetian et al., Phys. Rev. Lett. **87**, 182 001 (2001)
17. CLAS Collaboration, S. Stepanyan et al., Phys. Rev. Lett. **87**, 182 002 (2001)
18. K. Goeke, M.V. Polyakov, M. Vanderhaeghen, Prog. Part. Nucl. Phys. **47**, 401 (2001)
19. M. Diehl et al., Eur. Phys. J. C **39**, 1 (2005)
20. M. Guidal et al., Phys. Rev. D **72**, 054 013 (2005)
21. A.V. Radyushkin, Phys. Rev. D **59**, 014 030 (1999)
22. I.V. Musatov, A.V. Radyushkin, Phys. Rev. D **61**, 074 027 (2000)
23. M.V. Polyakov, C. Weiss, Phys. Rev. D **60**, 114 017 (1999)
24. F. Ellinghaus, PhD thesis, Humboldt University Berlin, Germany, January 2004, DESY-THESIS-2004-005
25. P.D.B. Collins, An Introduction To Regge Theory and High-Energy Physics (Cambridge, 1977)
26. LHPC Collaboration, P. Hägler et al., Eur. Phys. J. A **24S1**, 29 (2005)
27. QCDSF Collaboration, M. Göckeler et al., Few Body Syst. **36**, 111 (2005)
28. M. Diehl, A.V. Vinnikov, Phys. Lett. B **609**, 286 (2005)
29. A.D. Martin et al., Eur. Phys. J. C **4**, 463 (1998)
30. J. Pumplin et al., JHEP **0207**, 012 (2002)
31. A. Bacchetta et al., Phys. Rev. D **70**, 117 504 (2004)
32. V.A. Korotkov, W.-D. Nowak, Eur. Phys. J. C **23**, 455 (2002)
33. A.V. Belitsky, D. Müller, A. Kirchner, Nucl. Phys. B **629**, 323 (2002)
34. M. Diehl, S. Sapeta, Eur. Phys. J. C **41**, 515 (2005)
35. QCDSF Collaboration, M. Göckeler et al., Phys. Rev. Lett. **92**, 042 002 (2004)
36. HERMES Collaboration, F. Ellinghaus, Proc. 12th Int. Workshop on Deep-Inelastic Scattering, Štrbské Pleso, Slovakia, April 2004
37. J.C. Collins, L. Frankfurt, M. Strikman, Phys. Rev. D **56**, 2982 (1997)
38. M. Vanderhaeghen, P.A.M. Guichon, M. Guidal, Phys. Rev. D **60**, 094 017 (1999)
39. HERMES Collaboration, A. Airapetian et al., Eur. Phys. J. C **17**, 389 (2000)
40. A. Freund, M. McDermott, Eur. Phys. J. C **23**, 651 (2002)
41. A. Freund, M. McDermott, Phys. Rev. D **65**, 074 008 (2002)
42. L. Frankfurt, W. Koepf, M. Strikman, Phys. Rev. D **54**, 3194 (1996)
43. HERMES Collaboration, A.B. Borissov, Nucl. Phys. Proc. Suppl. **99A**, 156 (2001)
44. HERMES Collaboration, U. Elschenbroich, Proc. 11th Int. Workshop on Deep-Inelastic Scattering, St. Petersburg, Russia, April 2003